

Soft Matter

Accepted Manuscript



This is an *Accepted Manuscript*, which has been through the Royal Society of Chemistry peer review process and has been accepted for publication.

Accepted Manuscripts are published online shortly after acceptance, before technical editing, formatting and proof reading. Using this free service, authors can make their results available to the community, in citable form, before we publish the edited article. We will replace this *Accepted Manuscript* with the edited and formatted *Advance Article* as soon as it is available.

You can find more information about *Accepted Manuscripts* in the [Information for Authors](#).

Please note that technical editing may introduce minor changes to the text and/or graphics, which may alter content. The journal's standard [Terms & Conditions](#) and the [Ethical guidelines](#) still apply. In no event shall the Royal Society of Chemistry be held responsible for any errors or omissions in this *Accepted Manuscript* or any consequences arising from the use of any information it contains.

Polyethylene Glycol and Divalent Salt-Induced DNA Reentrant Condensation Revealed by Single Molecule Measurements

Chao Cheng, Jun-Li Jia, Shi-Yong Ran*

Department of Physics, Wenzhou University, Wenzhou 325035, China

Soft Matter Accepted Manuscript

* To whom correspondence should be addressed. E-mail: syran@wzu.edu.cn.

Abstract In this study, we investigated the DNA condensation induced by polyethylene glycol (PEG) with different molecular weights (PEG 600 and PEG 6000) in the presence of NaCl or MgCl₂ by magnetic tweezers (MT) and atomic force microscopy (AFM). The MT measurements show that with increasing NaCl concentration, the critical condensation force in PEG 600-DNA or PEG 6000-DNA system increased approximately linearly. PEG 6000 solution has a larger critical force than PEG 600 solution at a given NaCl concentration. In comparison, a parabolic trend of the critical condensation force was observed with increasing MgCl₂ concentration, indicating that DNA undergoes a reentrant condensation. The AFM results show that the morphologies of the compacted DNA-PEG complexes depended on the salt concentration and were consistent with the MT results.

Keywords: DNA reentrant condensation, PEG, single molecule, condensation force, magnetic tweezers

1. Introduction

Polyethylene glycol (PEG) is a neutral polymer with many applications ranging from industrial manufacturing to medicine. In the presence of salts, it can cause DNA condensation, and this process is also called polymer and salt-induced (psi) condensation or Ψ condensation.^{1,2} PEG has been widely used in medical field because of its nontoxic feature, solubility, and biocompatibility.^{3,4} It is also a useful vector to carry therapeutic DNA for gene delivery.⁵

The Ψ condensation was first reported by Lerman.⁶ This phenomenon has been widely studied by experimental⁷⁻¹⁸ and theoretical studies¹⁹⁻²³, and computer simulation.^{24,25} Vasilevskaya *et al.* studied the compaction of a single DNA molecule in the PEG solution by fluorescence microscopy.¹⁵ The critical concentration of PEG was found to decrease with increasing degree of PEG polymerization and salt concentration. Moreover, increasing concentration of high-molecular-weight PEG led DNA to undergo a reentrant globule–coil transition. Ramos *et al.* determined the critical concentration of PEG needed to induce condensation as a function of NaCl concentration.¹³ They also systematically studied the reentrant decondensation in PEG and univalent salt-induced DNA condensation and found a very strong dependence on the PEG molecular weight. At a low PEG molecular weight, decondensation occurs at relatively low concentrations of PEG and over

diverse salt concentrations. Froehlich *et al.* used Fourier transform infrared (FTIR), circular dichroism (CD), UV–visible, and atomic force microscopy (AFM) to study the binding of DNA with PEG of different molecular weights. The stability of the DNA complexes was in the following order: PEG 6000 > PEG 3350 > mPEG > anthracene.¹⁰ Kawakita *et al.* investigated the effect of the competition between the depletion and electrostatic interactions on the coil–globule transition and aggregate formation.¹¹ The globules coexist with the aggregates when the concentration of the unprobed DNA is higher than their overlap concentration. Hirano *et al.* investigated the kinetics of the compaction velocity of single DNA molecules in PEG and Mg^{2+} solution using fluorescence microscopy.⁹ The results show that the compaction velocity was proportional to the PEG concentration. Recently, Ojala *et al.* studied the PEG-induced DNA condensation in the presence of NaCl by optical tweezers and reported that PEG 1500 and PEG 4000 can condense DNA, whereas PEG 300 had no effect on the DNA condensation.⁷

The abovementioned studies indicate that the molecular weight of PEG and salt concentration play important roles in the Ψ condensation. However, to the best of our knowledge, the condensing ability of PEG on DNA has not been quantified, and this study can give a direct estimation of the Ψ condensation and promote the use of PEG in various fields. Moreover, very few studies have been focused on PEG and divalent

salt-induced DNA condensation, which should be different from PEG and univalent salt-induced system, because of the stronger electrostatic effect. In this study, the critical force of the DNA condensation in the PEG solution was measured in the presence of NaCl or MgCl₂ using the magnetic tweezers (MT) method. AFM was used to characterize the DNA-PEG complexes. The molecular weight and salt dependence of the DNA condensation were investigated. Interestingly, increasing Mg²⁺ concentration led to the reentrant DNA condensation.

2. Materials and methods

2.1 Materials PEG 600 and PEG 6000 [both 30% (w/v)] solutions in 100 mM Tris-HCl (pH=8.0) were purchased from Sigma-Aldrich and used as purchased to dissolve NaCl or MgCl₂ (Inalco-America Company (Beijing, China)). Bacterial λ-DNA (0.5 μg.μL⁻¹, 48,500 bp) and PBR322 DNA (1 μg.μL⁻¹, 4,361 bp) were purchased from New England Biolabs. The ends of λ-DNA were modified with 12 bp chemically labeled single-stranded oligonucleotides (3'-digoxigenin-tccagcggcggg and 3'-biotin-cccgccgctgga).²⁶ Magnetic beads coated with streptavidin (M-280, Dynal Biotech) were mixed with the modified DNAs for 30 min to form DNA-bead constructs. Distilled water was obtained from a Milli-Q system (Millipore, Billerica, MA, USA), and Tris-HCl buffer (100 mM, pH = 8.0) was used in all the preparations. NaCl or MgCl₂ was dissolved in PEG 600 or PEG 6000 solution to reach a final

concentration.

2.2 Methods

Magnetic tweezers measurement A transverse MT instrument was used to monitor the dynamic process of the end-to-end length of DNA and measure the critical force in the DNA condensation in room temperature (~ 25 °C). A 0.98×0.98 mm² glass capillary (Vitrocom, No 8270-50) was used as a flow cell. Inside the capillary, another thin capillary (Vitrocom, No. 5005-50) was glued on the inner surface. The sidewall of the thin capillary was coated with antidigoxigenin (Roche Diagnostics, Corp., Indianapolis, IN) to link the dig end of the DNA. Then, the DNA-bead constructs were flowed into the cell to form a side wall-DNA-bead structure (Fig. 1). The sample cell was placed on an inverted microscope. Then, the PEG solution in the presence of varying salt concentrations was loaded in the cell and incubated for about 10 min. During the loading, a permanent magnet controlled by a micromanipulator system (MP-285, USA) was used to stretch the DNA. In a typical measurement, the magnet was retracted at a constant speed of 11.294 $\mu\text{m/s}$, thus decreased the magnetic force on the suspending bead. The movement of the paramagnetic bead was recorded by a CCD in real time. The magnetic force (F) on the stretching DNA was measured according to the Brownian motion of the bead,^{27,28} and the distance (D) of the magnet to the paramagnetic bead was also measured (Fig. 1). With the

magnet moving at a constant speed from the same distance of the magnet to the paramagnetic bead, the length of DNA decreases smoothly with time. In the presence of PEG and the salt, the length of DNA abruptly decreases when condensation occurs (Fig. 2). According to the time of the critical point, the distance of the magnet to the paramagnetic bead can be calculated by the following formula:

$$D = D_0 + V \times T$$

where D_0 the starting distance of the magnet to the paramagnetic bead is 4,000 μm , V is the retracting speed of the magnet (11.294 $\mu\text{m} \cdot \text{s}^{-1}$), and T is the elapsed time at the critical condensation point. The critical force of the DNA condensation was obtained from Fig. 3.

To make sure that the measurements are reliable, the effects of viscosity of the PEG solutions and the retracting speed of the magnet were examined. Firstly, a latex bead ensemble with a known size (~ 200 nm in radius) in two PEG solutions were measured by dynamic light scattering method in order to infer the viscosity of the PEG solutions using Stokes-Einstein relation (Fig. S1). The measurements were did at 25 $^{\circ}\text{C}$. It was found that the viscosity of PEG 600 (30% w/v) is ~ 3.9 times of the viscosity of water, and the ratio is ~ 4.5 for PEG 6000 (30% w/v). The viscosity of the two solutions are very close and not so large to cause a long relaxation time. According to our estimation, a typical relaxation time for the DNA in the studied PEG solutions to achieve its

stable conformation is less than 2 seconds (Fig. S2). Therefore, it is reasonable to assume that the viscosity difference and the higher viscosity (compared with the viscosity of water) of the two PEG solutions do not affect the measurement of the critical condensation force. Secondly, for the chosen retracting speed of the magnet, a rough estimation can be made from the Force-Distance curve (Fig. 3). The movement of the magnet in ~ 2 s causes the force changing from 4.63 pN to 4.59 pN in the high force range, and the same displacement causes the force changing from 1 pN to 0.99 pN in the low force range. During a typical relaxation time period (less than 2 s) the change of the force is little enough (less than 0.04 pN) to rule out the effect of dynamic factor on the measurement. Considering all of these, it can be assumed that the chosen velocity is low enough to make sure that the measured force is not affected by the viscosity of the PEG solutions and other dynamic factors.

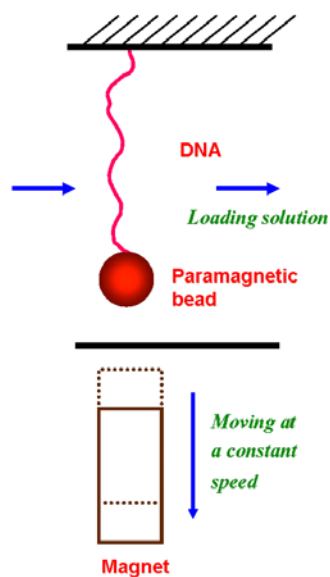


Fig. 1 Design of the MT experiment. PEG-salt solution was loaded into the channel and incubated with the suspending DNA molecule before the measurement begins. The magnet, exerting a force on the suspending DNA, was then moved at a constant speed of $11.294 \mu\text{m}\cdot\text{s}^{-1}$.

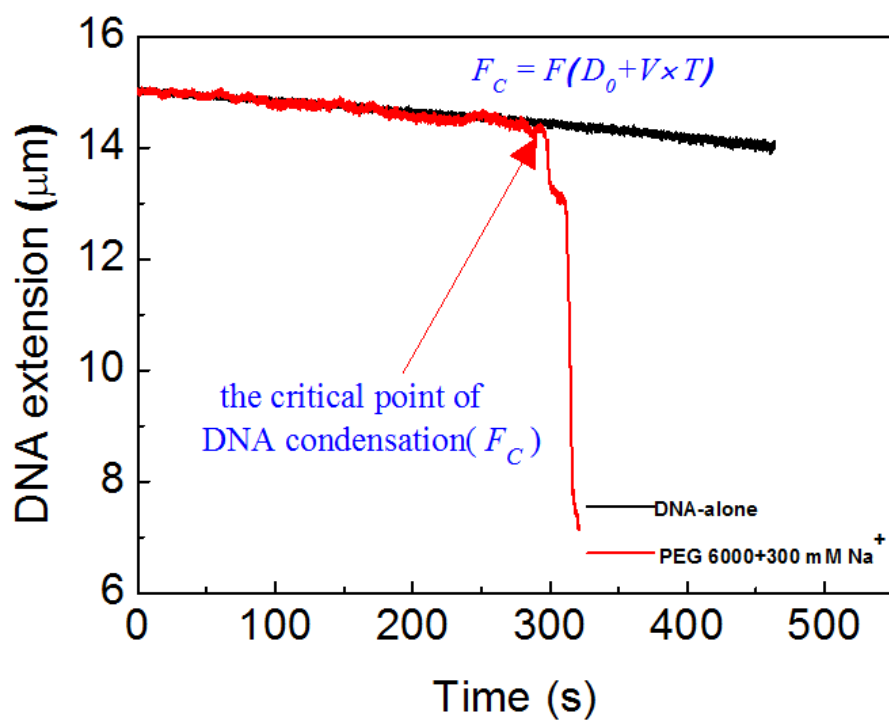


Fig. 2 Illustration of the critical condensation force (F_C) measurement. D_0 is the position of the starting magnet ($4,000 \mu\text{m}$). V is the velocity of the magnet ($11.294 \mu\text{m}\cdot\text{s}^{-1}$). T is the elapsed time at the critical point.

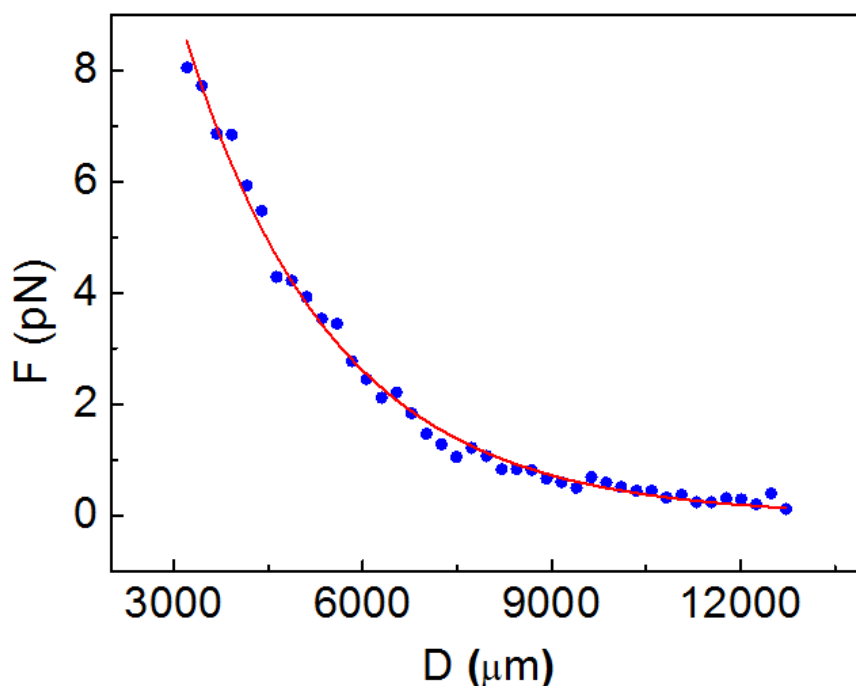


Fig. 3 Calibration of F–D relationship.

AFM imaging A SPM-9600 system (Shimadzu, Kyoto, Japan) was used to scan the DNA–PEG complexes in the presence of various concentrations of NaCl or MgCl₂. All samples were incubated overnight at room temperature (~25 °C). For each sample, the final concentration of DNA was 0.5 ng.μL⁻¹, and ~10 μL aliquot was deposited for 3 min on a freshly cleaved mica surface. The surface was rinsed with distilled water and dried using a gentle flow of nitrogen. AFM imaging was performed in the tapping mode at a resonance frequency of ~320 kHz.

3. Results

3.1 Critical force measurements We firstly checked the effect of the experimental buffer condition (100 mM Tris–HCl) on the condensation. It was found that without the addition of salts (Na⁺ or Mg²⁺), no detectable

transition can be found in PEG 600 solution (30% w/v) under the experimental buffer condition. To achieve a detectable transition, at least 300 mM Na⁺ was needed. In comparison, PEG 6000 solution alone can induce DNA condensation under the experimental buffer condition. By varying PEG 6000 concentration, it was found that the critical force decreased from the original ~0.6 pN at 30% PEG concentration to the final ~0.1 pN at 18% PEG concentration (Fig. 4). No detectable transition was found in PEG 6000 solutions with concentrations lower than 18%. It can be concluded that the added salts play important roles in the psi condensation. That is, without the presence of Na⁺ or Mg²⁺, the condensation cannot happen for PEG 600 system and the critical force could be lower than 0.6 pN for PEG 6000 system.

Next, the salt concentration dependence of the condensation was examined. Fig. 5 shows the critical force (F_C) of DNA condensation as a function of salt concentration (C) in PEG 600 (30% w/v) and PEG 6000 (30% w/v) solutions. For univalent salt solution, the forces approximately exhibit linear increasing trend for both the PEG 600 and PEG 6000 solution (Figs. 5A and 5B) in the studied range. In general, the PEG 6000 solution has a higher condensation force at a given salt concentration than the PEG 600 solution. The magnitude of the force could be as high as ~5 pN at 2 M NaCl concentration in the PEG 6000 solution compared to the force of ~2 pN in the PEG 600 solution. In comparison, the F_C increases

from a small value at a low MgCl_2 concentration, then reaches maximum at ~ 300 mM MgCl_2 in the PEG 600 solution and ~ 3 mM MgCl_2 in the PEG 6000 solution (Figs. 5C and 5D). The parabolic trend of the critical force in PEG- Mg^{2+} system indicates that DNA undergoes a reentrant condensation at higher MgCl_2 concentrations. To be specific, the reentrant condensation indicates that adding more salts inhibit DNA condensation, and consequently the complex structure at high salt concentrations is less compact compared to the condensate at the peak force point.

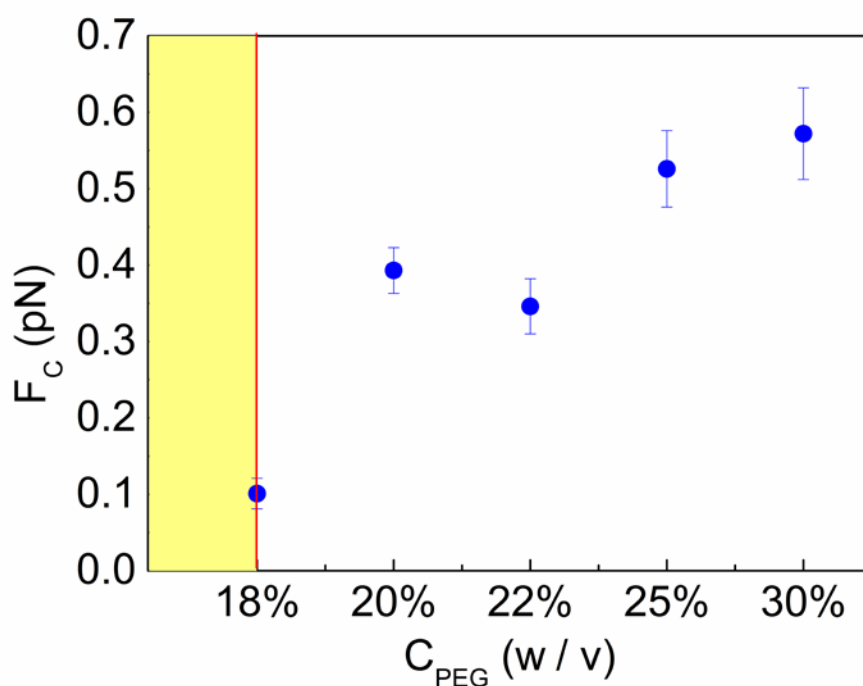
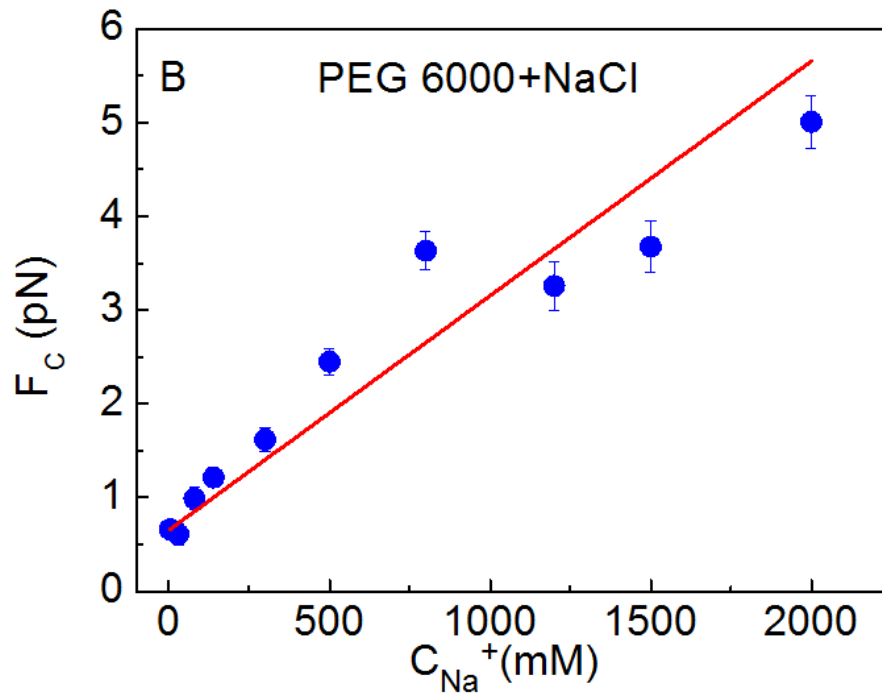
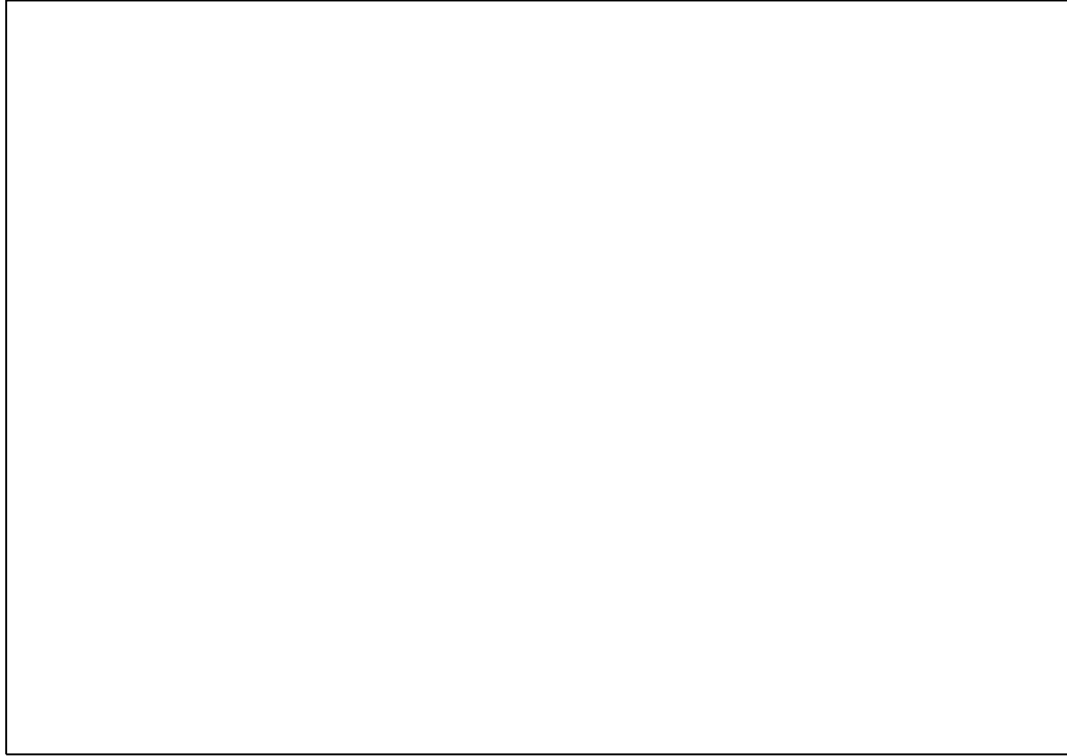


Fig. 4 The F_C of the DNA condensation as a function of the concentration of PEG 6000 solution (the used buffer is 100 mM Tris-HCl).



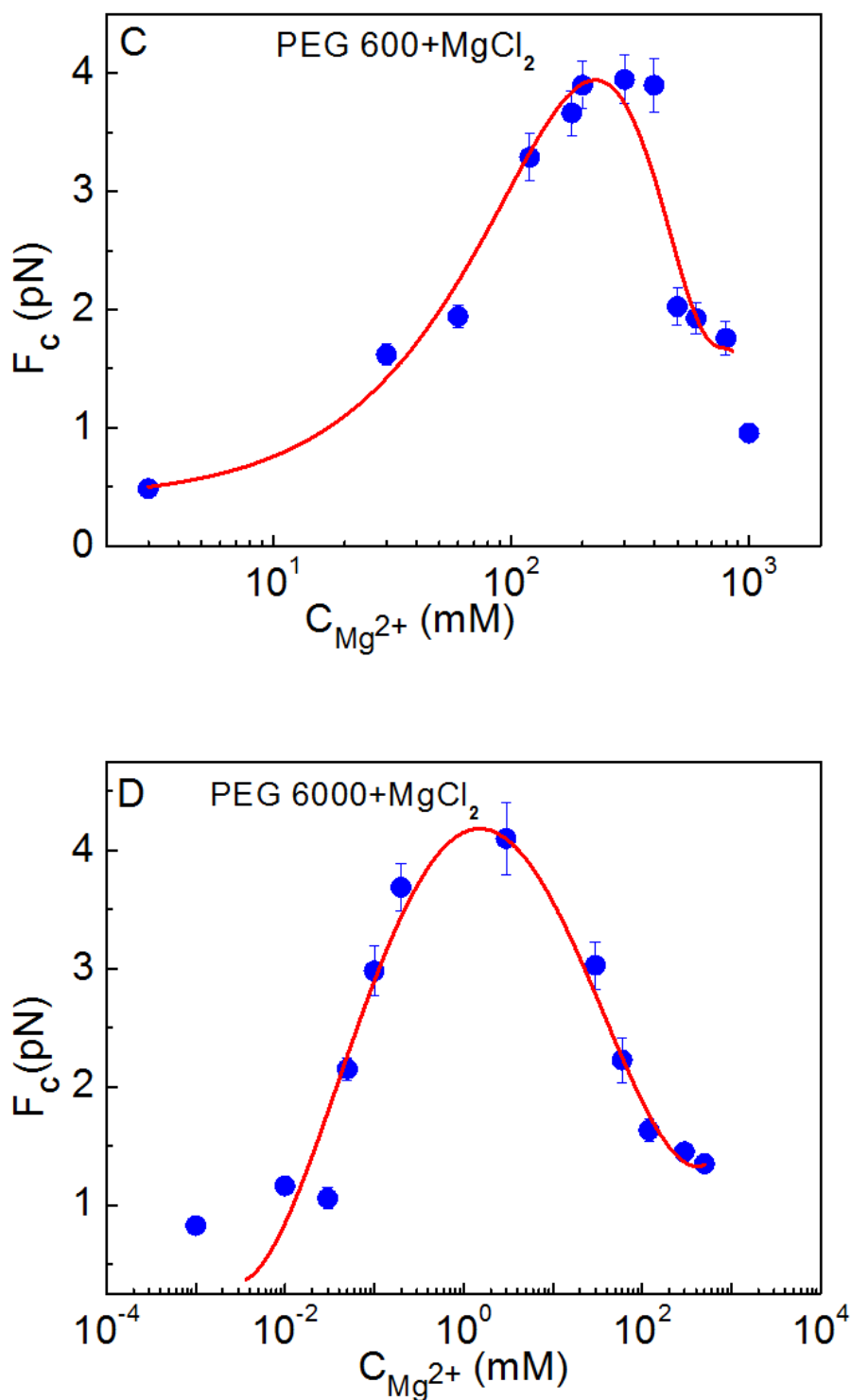


Fig. 5 The F_c of the DNA condensation as a function of salt concentration in PEG solution (30% w/v). A) PEG 600-NaCl system; B) PEG 6000-NaCl system; C) PEG 600-MgCl₂ system; and D) PEG 6000-MgCl₂ system. The error bars represent the inaccuracies result from the distance measurements and other factors. The data in A) and B) were fitted using a linear function, and a polynomial function was used to fit the data of C) and D).

3.2 Morphology characterization by AFM To make sure that DNA

reentrant condensation exists in PEG-Mg²⁺ system, AFM was used as an auxiliary method to characterize the λ -DNA-PEG complexes (Figs. 6 and 7). In fact, the height of the complex is an indicator of its compactness. If the complex is incompact to some degree, then a lower height of the complex in AFM characterization should be expected.

Fig. 6 shows the typical images of the λ -DNA condensates at varying magnesium salt concentrations in the PEG-6000 solution. The height of a typical condensate at 0.01 mM Mg²⁺ is ~15 nm. Increasing salt concentration first increases the height to a maximum of ~30 nm at 30 mM Mg²⁺ and then decreases further. Fig. 7 shows the statistics of the heights of the condensates as a function of Mg²⁺ concentration. Obviously, the parabolic trend of the measured height is consistent with the critical force measurements and also supports the existence of the DNA reentrant condensation in PEG-Mg²⁺ system.

The condensing force difference of the two PEG solutions shown in the MT measurements is also demonstrated by the AFM characterization. Fig. 7 shows the typical images of the DNA condensates in the PEG 600 solution. Compared to the PEG 6000 system, the complexes in the PEG 600 solution show profiles lower than 10 nm, indicating that PEG 600 cannot condense DNA with a high compactness as that of PEG 6000.

One might concern that if this reentrant condensation is common for the condensation of other DNA. Then, another DNA called PBR322

with a shorter length (4,361 bp) was used in AFM characterization. Fig. 9 shows some representative images of PBR322 DNA condensates in the PEG 6000 solution with varying magnesium salt concentrations. Profile measurements show that the typical height of the complexes are ~ 2.8 nm, ~ 17.8 nm, ~ 2.0 nm and ~ 1.2 nm, and the corresponding MgCl_2 concentrations are 0.1 mM, 5 mM, 300 mM and 500 mM, respectively. Fig. 10 further gives the statistics of the heights of the condensates as a function of Mg^{2+} concentration. Again, increasing Mg^{2+} leads to the decreasing height of the complexes, which suggests the same behavior as observed in Fig. 6. Therefore, it is reasonable to believe that the reentrant behavior is common in the Ψ condensation caused by PEG and Mg^{2+} .

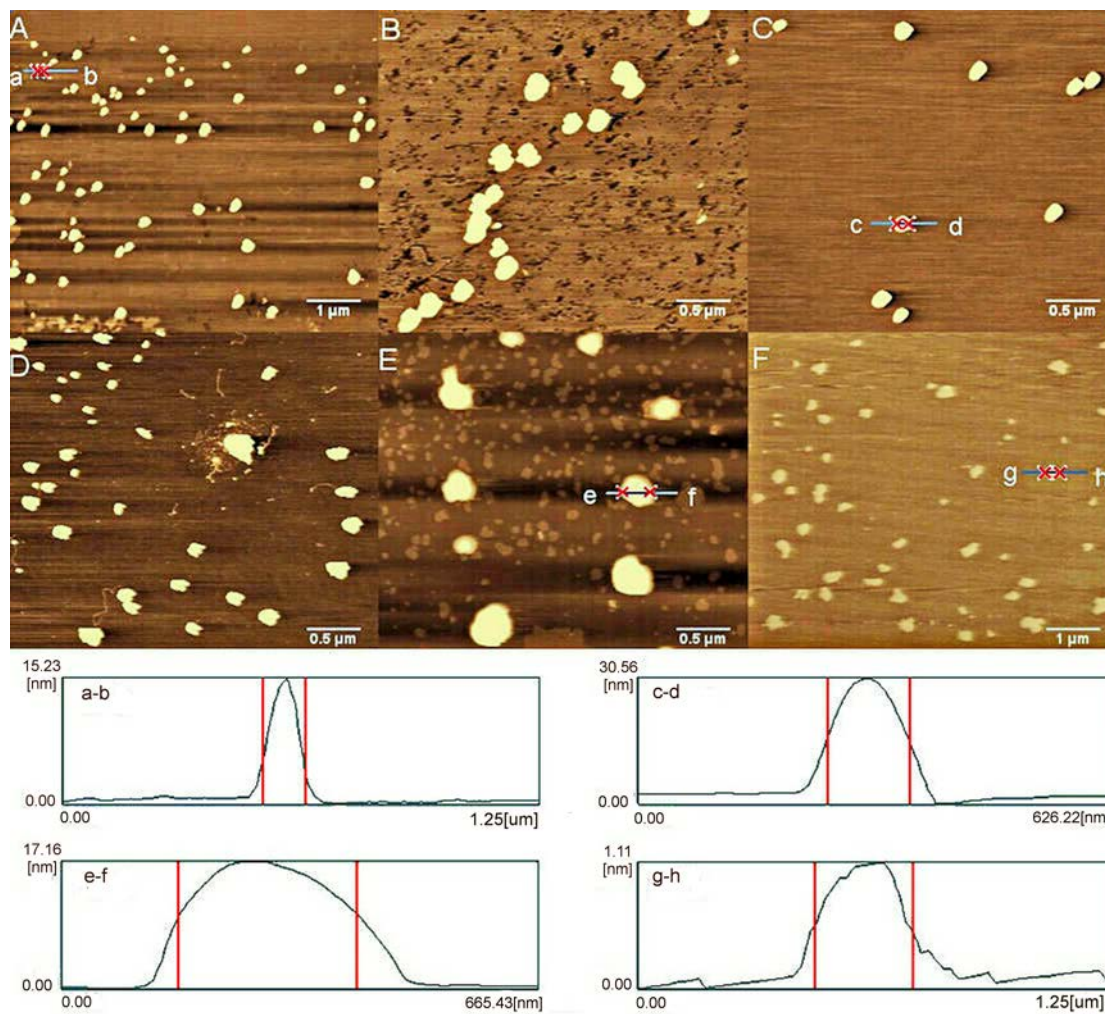


Fig. 6 Typical images of DNA condensates in PEG-6000 solution (30% w/v) under varying $MgCl_2$ concentrations. From A to F, the $MgCl_2$ concentrations are 0.01, 3, 30, 300, 500, and 1,000 mM. The corresponding typical profile measurements are shown in the bottom part of the figure.

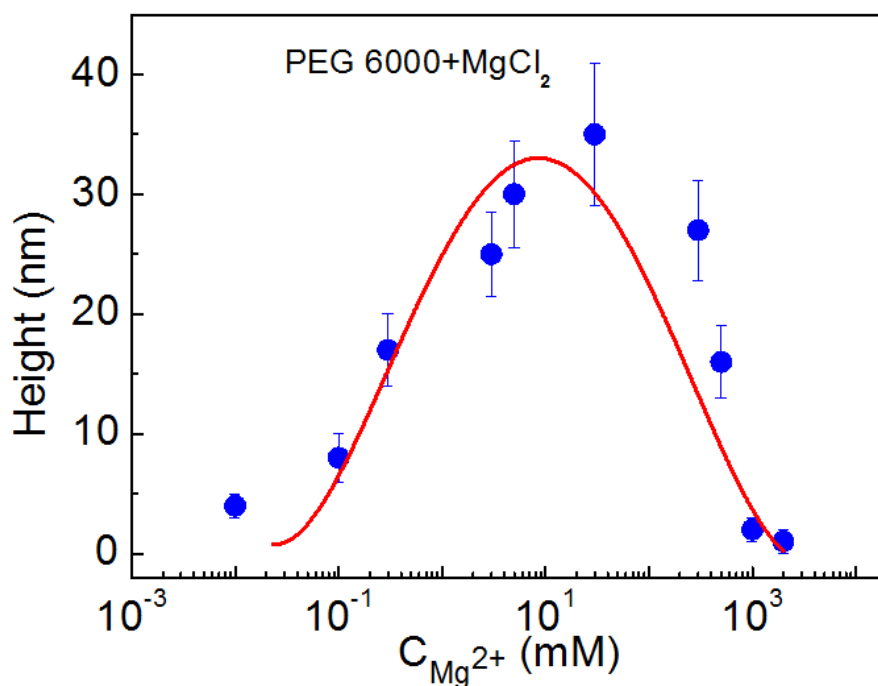


Fig. 7 The statistical height of the DNA-PEG complexes as a function of $MgCl_2$ concentration (~ 0.001 – $2,000$ mM) in the PEG-6000 solution (30% w/v). The error bars represent the standard deviation of the average of ten measurements. The data was fitted using a polynomial function.

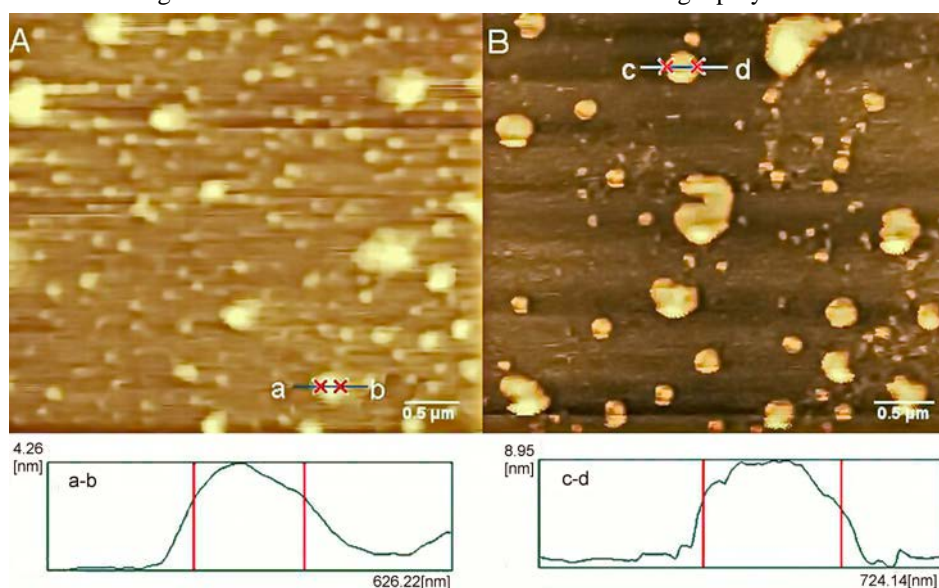


Fig. 8 Typical images of the PEG 600-induced DNA complexes under different salt conditions. A) 800 mM NaCl; B) 3 mM $MgCl_2$. The heights of the measured complexes in Figs. 8 A) and B) are ~ 4 and 9 nm, respectively.

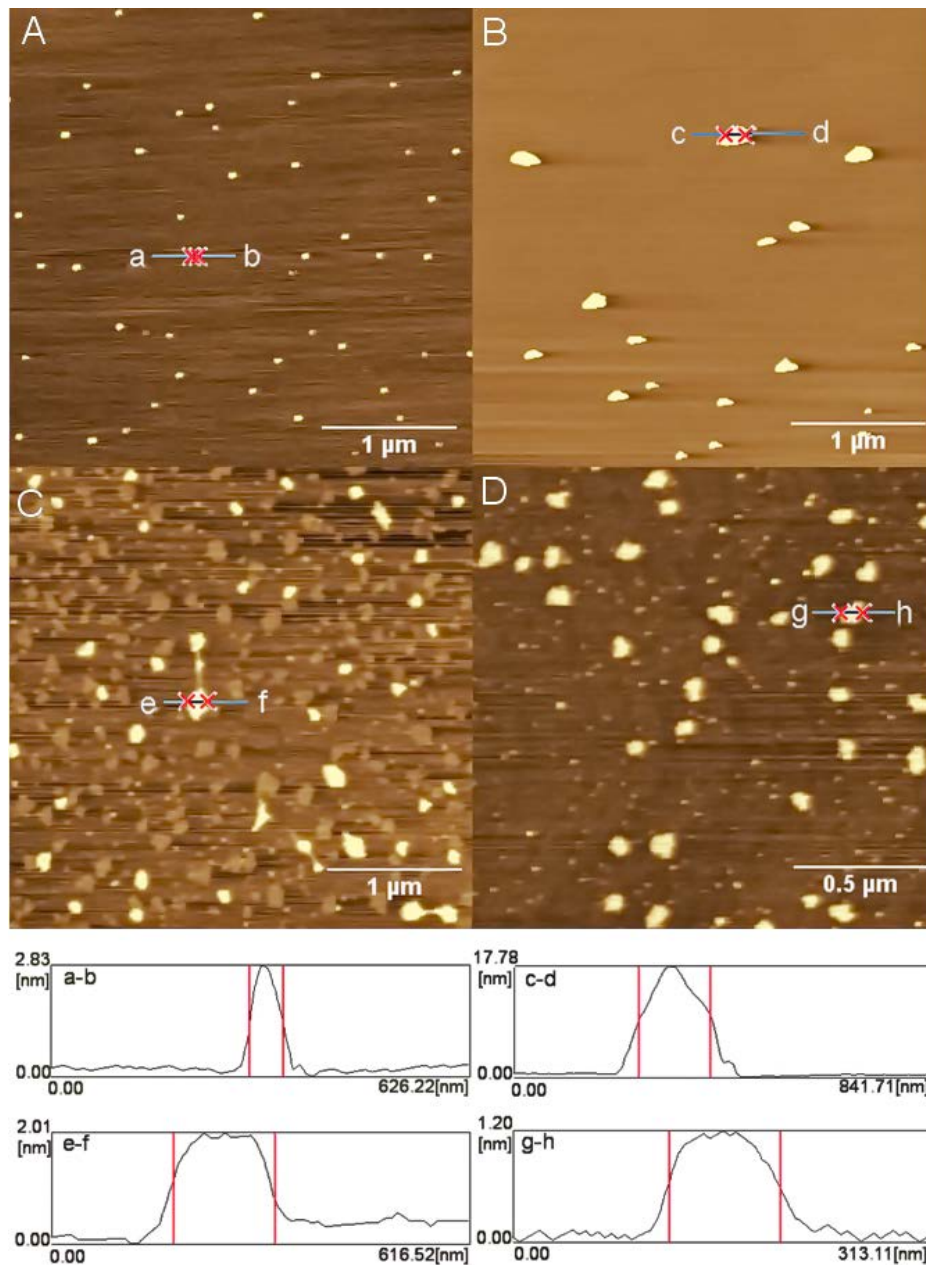


Fig. 9 Typical images of PBR322 DNA condensates in PEG-6000 solution (30% w/v) under varying $MgCl_2$ concentrations. From A to D, the $MgCl_2$ concentrations are 0.1, 5, 300 and 500 mM. The corresponding typical profile measurements are shown in the bottom part of the figure.

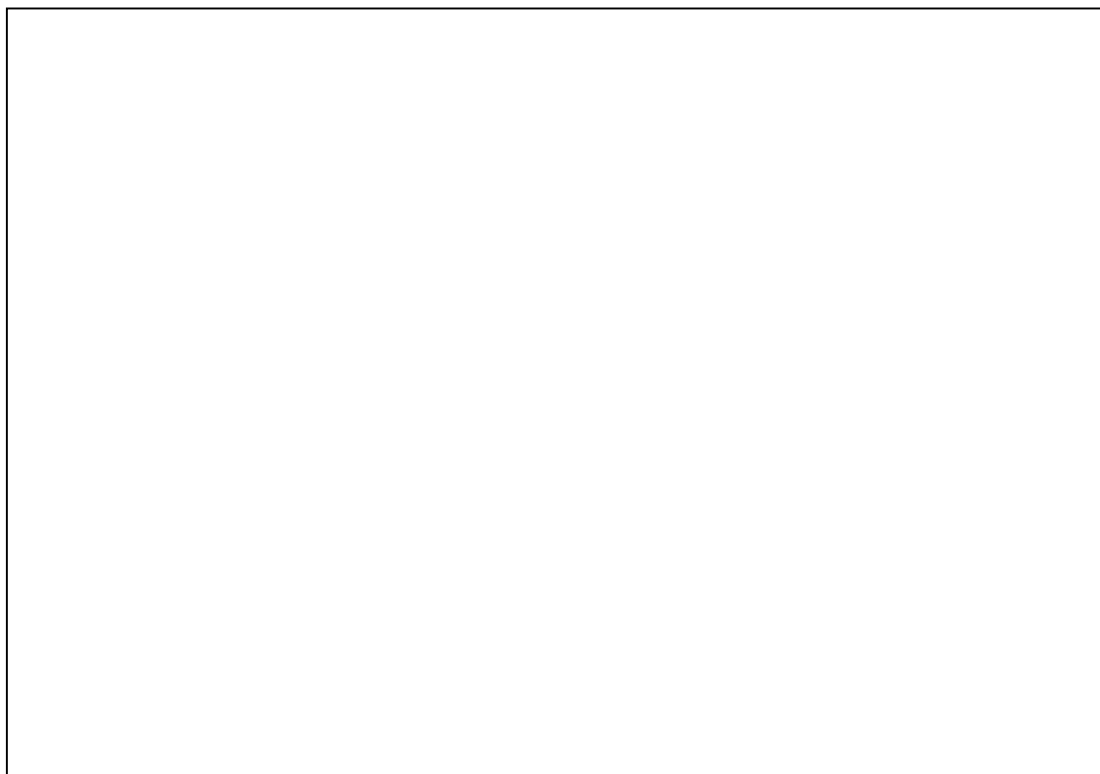


Fig. 10 The statistical height of the PBR322 DNA-PEG complexes as a function of MgCl_2 concentration (~ 0.01 – $2,000$ mM) in the PEG-6000 solution (30% w/v). The error bars represent the standard deviation of the average of ten measurements.

4. Discussion

4.1 Condensation mechanism Force is an important factor in DNA-related processes.^{29,30} The MT measurements are actually a competition between the external energy and the condensation free energy. As shown in Fig. 11, if the external force (F) is lower than the condensation free energy per unit DNA length ($-\Delta g$), the condensation occurs. If F is approximately equal to or larger than $-\Delta g$ for uncompact DNA, DNA chain remains in its original conformation. For the compacted DNA, exerting a larger force ($F > -\Delta g$) could unravel the complex.

As shown in the above measurements, for univalent ion buffer, adding

more salts increases the critical force and is attributed to the role of the salt ions in the Ψ condensation. The added salts can neutralize the charges of DNA and consequently decrease the electrostatic resistance between different DNA parts; however, the depletion forces of the polymer tend to push different DNA parts together. Considering the roles played by PEG and salt, it is understandable that PEG can overcome a higher force barrier for the condensation to occur at higher salt concentrations, because of strengthened screening effect.

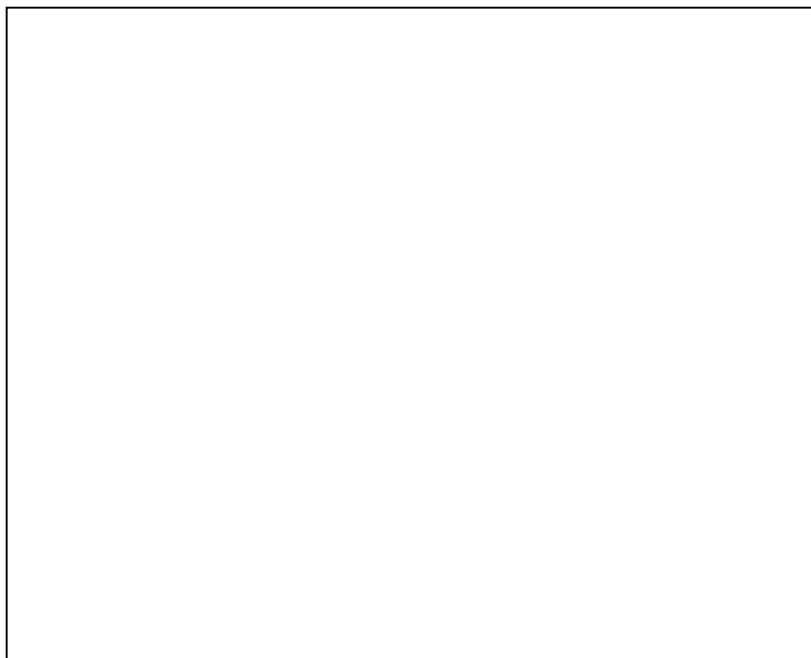
Molecular weight is another important factor in the present Ψ condensation. PEG is a flexible polymer, and its crowding effect can facilitate the looping of DNA and further induce DNA condensation.²⁵ For a given PEG concentration, measurements show that low-molecular-weight PEG has a higher osmotic pressure.³¹ Therefore, higher osmotic pressure should not be the reason for the higher condensing ability of PEG 6000. However, the free energy of transferring a DNA molecule from a dilute solution into a concentrated solution of flexible polymers can be expressed by the following equation :

$$\Delta G_{free} \cong \Pi_{crowd} \cdot V_{exlu} ,$$

where Π_{crowd} is the osmotic pressure of the polymer, and V_{exlu} is the volume around the DNA cylinder from which polymers segments are excluded or depleted.¹ Because the osmotic pressure difference is not the reason for the condensation difference in the two PEG solutions, it is

reasonable to suggest that the exclusion volume of PEG 6000 is higher than that of PEG 600.

The salt and molecular weight dependence of the Ψ condensation can provide a guidance to control the compactness of the PEG–DNA complexes used in gene delivery. Based on this study, the adding of high-molecular-weight PEG and divalent salt induced DNA condensate with a high compactness.



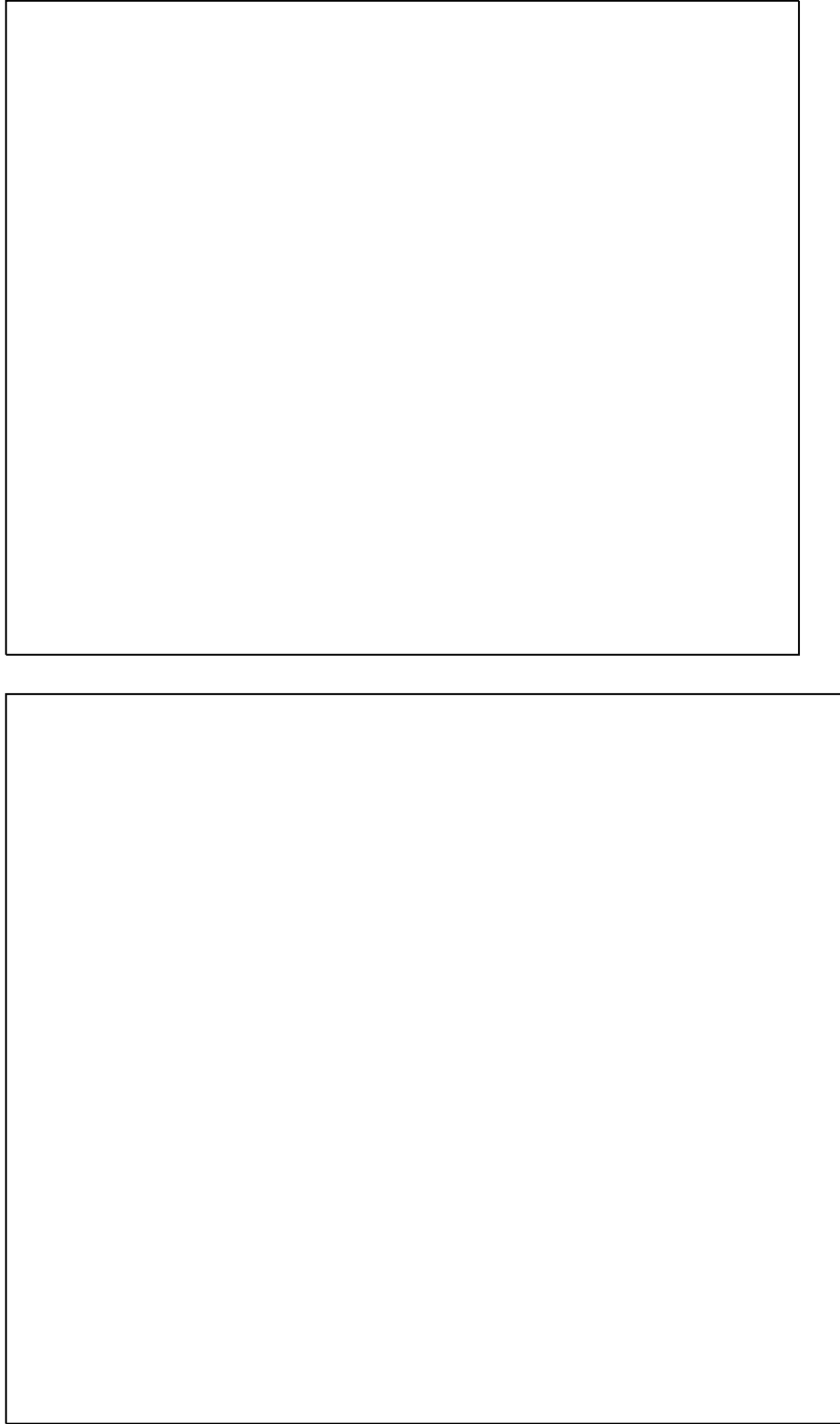


Fig. 11 Some representative curves in MT measurements under different constant forces. The loaded solution is PEG 6000 + 140 mM NaCl. F is the exerted force, $-\Delta g$ is the condensation free energy per unit DNA length. A) $F < -\Delta g$; B) $F \sim -\Delta g$; C) $F > -\Delta g$.

4.2 Reentrant condensation To the best of our knowledge, the reentrant behavior in the Ψ condensation by increasing Mg^{2+} concentration is the

most striking feature of this study and has not been reported before. Nevertheless, the DNA reentrant condensation in multivalent ions solution has been reported in previous studies.³²⁻³⁸ Therefore, it would be necessary to compare the present finding with the multivalent ion-induced DNA reentrant condensation. For the latter reentrant phenomenon, Besteman *et al.* suggested that the charge inversion is the main criteria.³⁴ The main interpretation of their experimental study was that when a polyelectrolyte is neutralized to carry sufficient low effective charges, the electrostatic correlation overcoming the electrostatic repulsion leads to the condensation. However, when the effective charge of the polyelectrolyte is reversed, the electrostatic repulsion is dominant again, and then the reentrant condensation occurs. Their condensation force measurements agreed well with the counterion correlation theory prediction.^{37,38} Interestingly, Todd *et al.* provided another possible explanation of the same phenomenon.^{32,33} They reported that the reentrant condensation occurs near the solubility limit of the multivalent cation salt. Near this limit, the formation of lower-valent anion-associated multivalent cations is more likely, thus increasing the energy cost for neutralizing DNA. For example, trivalent cations associate with univalent anions and form divalent ion pairs. Apparently, the divalent ion pairs have lower condensing ability than the multivalent ions; therefore, it is understandable that a high concentration of multivalent cation decreases

the DNA condensation force.

We believe that the ion pair formation is not the reason for the reentrant behavior presented in this study. MgCl_2 has a high solubility; and in the studied concentration range, the ion pair effect is negligible. The electrophoretic mobility of the complexes was also measured using the dynamic light scattering method to ascertain whether the charge inversion occurs. However, it was not successful, because the high salt concentration resulted in a high electrochemical current, hence the output results are not meaningful. Despite the failure, electrostatic interaction surely plays an important role in the reentrant behavior, and the charge inversion is still a possible reason. Moreover, according to the electrostatic correlation theory, divalent ions have a weak correlation effect compared to the ions with higher valence. Whether the presence of crowding polymers strengthens the correlation effect remains to be investigated theoretically.

The electrostatic zipper theory, describing the details of the surface charge pattern, determines the specificity and energetics of the DNA condensation and may be another possible mechanism to explain the present finding.³⁹ The main point of this theory is the binding of cations in helical grooves, resulting in the axial charge separation, which allows the attraction between the opposite charges along the DNA–DNA contact and forms an electrostatic zipper-like structure. This theory also suggests

that temperature-favored DNA aggregation is ascribed to Mn^{2+} repartitioning between the binding sites in the minor and major grooves.⁴⁰ Analogously, Mg^{2+} may redistribute between the minor and major grooves with increasing Mg^{2+} concentration in the presence of PEG. If this redistribution breaks the electrostatic zipper-like structure to some degree, the attraction between the DNA parts may not be favored, leading to the reentrant condensation.

4.3 AFM characterization assessment The reentrant condensation behavior has been reported to be the resolubilization phenomenon in bulk experiment. Pelta *et al.* studied the polyamine and cobalthexamine-induced DNA condensation by measuring the amount of uncondensed DNA in the supernatant.⁴¹ They reported that adding multivalent cations first leads to the DNA precipitation; further addition leads to the resolubilization of the DNA condensates and was verified by the increased DNA concentration in the supernatant. The present AFM scanning was also based on the measurement of the DNA condensates in bulk solution. It is reasonable to assume that resolubilization decreases the size and compactness of the DNA condensate. Therefore, this phenomenon should be reflected in the present AFM height characterization, because the measured height is related to the two properties. In other words, the resolubilization behavior also occurred in this Ψ condensation, as shown in Fig. 7.

4.4 Comparison with previous studies Vasilevskaya *et al.* reported that the critical concentration of PEG decreases with increasing degree of PEG polymerization and salt concentration.¹⁵ This positive correlation is consistent with the univalent salt and molecular weight dependence of the critical force in the present Ψ condensation. The measured critical concentration of 18% in Fig.4 is comparable to the ~25% concentration of PEG 8000 in their research considering that the concentration of Tris-HCl (100 mM) of this study is higher than the concentration (10 mM) in the reference. However, it should be noted that the single method used in this study cannot detect the coexistence of coil conformation and globule conformation because it can only measure one DNA molecule, which may be another reason to cause the critical concentration difference of the two studies. Moreover, increasing concentration of high-molecular-weight PEG leading DNA to undergo a reentrant globule–coil transition has been reported previously.^{13,15} Ramos *et al.* further suggested that in the reentrant decondensation the flexible polymers used are not completely excluded from the condensed phase. The reentrant behavior is similar to the behavior observed in this study. However, it is important to note that the concentration of PEG was not changed in the present measurements, and only the salt conditions were changed. Therefore, the difference between the two reentrant behaviors still needs detailed investigation.

5. Conclusions

We investigated the DNA condensation by PEG in the presence of univalent or divalent salt using the MT and AFM methods. In the studied concentration range, the measurements show that with increasing NaCl concentration, the critical condensation force in the PEG 600-DNA or PEG 6000-DNA system increased approximately linearly. The PEG 6000 solution has a larger critical force than the PEG 600 solution at a given univalent salt concentration. In comparison, a parabolic trend in the critical condensation force with increasing MgCl_2 concentration was observed for MgCl_2 , indicating that the Ψ condensation also shows the reentrant behavior. The AFM characterization also supported the finding and indicated that the reentrant condensation is reflected to be the resolubilization phenomenon.

6. Acknowledgments.

This work was supported by the Natural Science Foundation of China (No.21204065, 20934004) and the Zhejiang Provincial Natural Science Foundation of China (No.Y4110357).

7. References

1. R. de Vries, *Biochimie*, 2010, **92**, 1715-1721.
2. V. A. Bloomfield, *Current opinion in structural biology*, 1996, **6**, 334-341.
3. B. Obermeier, F. Wurm, C. Mangold and H. Frey, *Angewandte Chemie International Edition*, 2011, **50**, 7988-7997.
4. J. V. Jokerst, T. Lobovkina, R. N. Zare and S. S. Gambhir, *Nanomedicine*, 2011, **6**, 715-728.
5. D. D. Lasic, *Liposomes in gene delivery*, CRC press, 1997.
6. L. Lerman, *Proceedings of the National Academy of Sciences*, 1971, **68**, 1886-1890.

7. H. Ojala, G. Ziedaite, A. E. Wallin, D. H. Bamford and E. Hægström, *European Biophysics Journal*, 2014, **43**, 71-79.
8. W. Xu and S. J. Muller, *Lab on a chip*, 2012, **12**, 647-651.
9. K. Hirano, M. Ichikawa, T. Ishido, M. Ishikawa, Y. Baba and K. Yoshikawa, *Nucleic acids research*, 2012, **40**, 284-289.
10. E. Froehlich, J. Mandeville, D. Arnold, L. Kreplak and H. Tajmir-Riahi, *The Journal of Physical Chemistry B*, 2011, **115**, 9873-9879.
11. H. Kawakita, T. Uneyama, M. Kojima, K. Morishima, Y. Masubuchi and H. Watanabe, *The Journal of chemical physics*, 2009, **131**, 094901.
12. T. Saito, T. Iwaki and K. Yoshikawa, *Chemical Physics Letters*, 2008, **465**, 40-44.
13. J. É. B. Ramos, R. de Vries and J. Ruggiero Neto, *The Journal of Physical Chemistry B*, 2005, **109**, 23661-23665.
14. K. Yoshikawa, Y. Yoshikawa, Y. Koyama and T. Kanbe, *Journal of the American Chemical Society*, 1997, **119**, 6473-6477.
15. V. Vasilevskaya, A. Khokhlov, Y. Matsuzawa and K. Yoshikawa, *The Journal of chemical physics*, 1995, **102**, 6595-6602.
16. H. Frisch and S. Fesciyan, *Journal of Polymer Science: Polymer Letters Edition*, 1979, **17**, 309-315.
17. T. Maniatis, J. H. Venable and L. S. Lerman, *Journal of molecular biology*, 1974, **84**, 37-64.
18. K. Minagawa, Y. Matsuzawa, K. Yoshikawa and A. Khokhlov, *Biopolymers*, 1994, **34**, 555-558.
19. R. de Vries, *Biophysical journal*, 2001, **80**, 1186-1194.
20. C. B. Post and B. H. Zimm, *Biopolymers*, 1982, **21**, 2123-2137.
21. A. Y. Grosberg, I. Y. Erukhimovitch and E. Shakhnovitch, *Biopolymers*, 1982, **21**, 2413-2432.
22. C. B. Post and B. H. Zimm, *Biopolymers*, 1979, **18**, 1487-1501.
23. J. Naghizadeh and A. Massih, *Physical Review Letters*, 1978, **40**, 1299.
24. J. Shin, A. G. Cherstvy and R. Metzler, *Soft matter*, 2015, **11**, 472-488.
25. J. Shin, A. G. Cherstvy and R. Metzler, *ACS Macro Letters*, 2015, **4**, 202-206.
26. S. B. Smith, L. Finzi and C. Bustamante, *Science*, 1992, **258**, 1122-1126.
27. S.-Y. Ran, Y.-W. Wang, G.-C. Yang and L.-X. Zhang, *The Journal of Physical Chemistry B*, 2011, **115**, 4568-4575.
28. T. Strick, J.-F. Allemand, D. Bensimon, A. Bensimon and V. Croquette, *Science*, 1996, **271**, 1835-1837.
29. J. Shin, A. G. Cherstvy and R. Metzler, *Physical Review X*, 2014, **4**, 021002.
30. C. Bustamante, Z. Bryant and S. B. Smith, *Nature*, 2003, **421**, 423-427.
31. N. M. Iraki, R. A. Bressan, P. Hasegawa and N. C. Carpita, *Plant Physiology*, 1989, **91**, 39-47.
32. B. A. Todd and D. C. Rau, *Nucleic acids research*, 2008, **36**, 501-510.
33. B. A. Todd, V. A. Parsegian, A. Shirahata, T. Thomas and D. C. Rau, *Biophysical journal*, 2008, **94**, 4775-4782.
34. K. Besteman, K. Van Eijk and S. Lemay, *Nature Physics*, 2007, **3**, 641-644.
35. E. Allahyarov, G. Gompper and H. Löwen, *Journal of Physics: Condensed Matter*, 2005, **17**, S1827.
36. A. Y. Grosberg, T. Nguyen and B. Shklovskii, *Reviews of modern physics*, 2002, **74**, 329.
37. B. I. Shklovskii, *Physical Review E*, 1999, **60**, 5802.

38. T. T. Nguyen and B. I. Shklovskii, *The Journal of Chemical Physics*, 2001, **114**, 5905-5916.
39. A. Kornyshev and S. Leikin, *Physical review letters*, 1999, **82**, 4138.
40. A. G. Cherstvy, A. A. Kornyshev and S. Leikin, *The Journal of Physical Chemistry B*, 2002, **106**, 13362-13369.
41. J. Pelta, F. Livolant and J.-L. Sikorav, *Journal of Biological Chemistry*, 1996, **271**, 5656-5662.